Research Article – Vol. 01, Issue 04, No. 05

Advanced in Engineering and Intelligence Systems

Journal Web Page: https://aeis.bilijipub.com

Estimating the Pile Settlement Using a Machine Learning Technique Optimized by Henry's Gas Solubility Optimization and Particle Swarm Optimization

Saravana Kumar, M [1,*] Savarimuthu Robinson [2]

[1] *Department of Mechanical Engineering, Mount Zion College of Engineering and Technology, Pudukottai, Tamilnadu 622507, India*

[2] *Department of Electronics and Communication Engineering, Mount Zion College of Engineering and Technology, Pudukkottai, 622507, Tamil Nadu, India*

Highlights

- *A rich dataset of pile settlements is gathered from various kinds of literature.*
- *A pre-process was implemented to prepare the dataset.*
- *A robust model is developed based on support vector regression.*
- *The robustness of the model improved by coupling the model with Henry's gas and particle swarm optimization algorithms.*

Article Info

Received: 06 November 2022
Received in revised: 30 December 2022
Accepted: 30 December 2022
Available online: 01 January 2023

Keywords

Pile Settlement;
Support vector regression;
Henry's Gas SolubilityOptimization;
Particle Swarm Optimization;
Machine learning.

Abstract

Ensuring constructional projects are safe, like stacked structures, requires consideration to immunize structures over the period. Pile settlement (PS) is an important project problem and is receiving a lot of attention to prevent failure before construction starts. Several items for estimating pile motion can help understand the project's perspective during the loading phase. Most intelligent strategies for the mathematical calculation of pile movement are used in PS simulations. Therefore, in present article, a developed framework operating support vector regression (SVR) together with Henry's Gas Solubility Optimization (HGSO) and Particle Swarm Optimization (PSO) was considered for accurate pile motion calculation. The usages of optimizers were to tune some internal settings of SVR. The Kuala Lumpur transportation network was selected to study the movement of piles based on the land rock characteristics using the developed SVR-HGSO and SVR-PSO structures. Five metrics were used to evaluate the performance of each model. The main objective of this research is to evaluate the artificial inteligent approach in form of two developed models in simulating the pile settlement rates using hybrid optimized frameworks. The R^2 of modeling both were obtained similarly at 0.99 level. While the RMSE of SVR-PSO appeared more than two-fold of SVR-HGSO, 0.46 and 0.29 mm, respectively. Also, test phase results showed the better performance of SVR-HGSO with an MAE index of 0.278, which is 57.10% lower than the other one. The OBJ proved accurate modeling by SVR-HGSO calculated at 0.283mm level.

1. Introduction

Several studies carried out to calculate the response of piles to feasible axial loads are discussed in lectures with the help of related studies [1,2]. Existing knowledge of how piles respond under load has led to improvements in many strategies that researchers can use to evaluate pile motion. Several researchers in this field referred to the strategies mentioned at the time, especially studies such as [3,4]. Mentioned methods range from calculation methods in an easy way, using analytical and practical solutions, even by utilizing finite element or numerical difference solutions [5–7]. Empirically, simultaneously designing the premise of methods for the pile to be primarily based totally in a layer underneath the soil followed with the aid of a much less compressible layer [8–11].

Therefore, the compression layers under the piles were generally accepted as this is an obvious design issue and risk as it can significantly increase pile settlement [12]. One study [13] suggests an additional subsidence rate due to beneath layers, which may be important to pile geometry

* Corresponding Author: Saravana Kumar, M
Email: m.saravanakumar@mountzioncollege.org

and soil physical properties, depending on the limited analysis. Research into this seemingly, the obvious classic question is limited, and manual calculations and methods that appear analytically are often not applicable to existing individual soil layers.

In addition, another study suggested a method to analyze the mobility of piles and introduce a theoretical function for the study of earth pressure coefficient [14,15]. All references primarily evaluate the motion of piles, but anyone is utilized without a ground reflection model directly. Also, solutions are known as artificial neural networks (ANN) and properly branched machine learning is the result of a lot of research, Lee and Lee [16], Che et al. [17], Liu et al. [18], Hanna et al. [19], and Shanbeh et al. [20]. In several studies, training data augmentation was chosen to generate models capable of predicting pile bearing capacity and movement tests that data collection selected training samples with respect to neural networks in a series of dynamic field studies. One research that operated ANN tried to calculate the settlement characteristics of piles socketed in rocks. That dataset for the training phase was collected via the reports of actual piles data [21].

Regression methods have been widely used, such as multivariate spline adaptive regression, Gaussian trend regression, and minimax probability machine regression [22–25,10,26,27]. Solving problems in geotechnical fields is examined through gene expression programming (GEP) [26,28–31]. This method of determining the axial bearing capacity of piles has been studied in several types of research [28]. A new configuration according to GEP has been progressed [29]. Algorithms performed other research to predict the UCS of rocks [31], including support vector machines, GEP, and multilayer perceptrons. The ability of support vector machines to simulate the motion of stratified sedimentary rock masses is quite acceptable [32]. Actually, the support vector machine provides more accurate and reliable calculation outcomes. Moreover, in other studies, this method was used to evaluate the bearing capacity of piles [33,34]. Input data included empirical or field-measured soil properties, foundation sizes, and pile samples.

The main aim of the present paper is to appraise the pile settlement rates socketed in rocks by applying support vector regression (SVR) to develop a practical pile movement model. In this regard, this article attempted to combine, promote, and explore relevant models with optimization algorithms and SVR machine learning to estimate pile settlement rates based on in-situ data. SVR used algorithms including Henry's Gas Solubility Optimization (HGSO) and Particle Swarm Optimization (PSO) to reach these goals to find optimal coefficient values related to the models and improve simulation accuracy. There are many references using SVR and optimization algorithms in literature [35–40]. Practical data to analyze pile motion and soil attributes were gathered from the Kuala Lumpur Transport Klang Valley Rapid Network (KVMRT) project in Malaysia.

The frameworks proposed as SVR-HGSO and SVR-PSO attempt to simulate the pile settlement rates by the dataset. Generally, developing boosted models such as hybrid and ensemble ones can lift the capabilities of them in tunning the main predicting models while some experts have great tendency for hybrid than ensemble [41]. In fact using artificial intelligent-based techniques are getting common in civil engineering fields to save invests, energy, at the same time, increasing the accuracy of predictions. In this regard, the parameters of the ratio of pile length to its diameter, the UCS explored in rock, the pile loads, the ratio of pillar length beneath the soil to the length of the pile in the rock, as well as the N_{SPT} parameters, penetration test, were opted to examine the pile settlement in the project of KVMRT [42]. On the other hand, investigating the reliability of the models proposed requires the evaluators that in the present study, the criteria of R, OBJ, MAE, and RMSE as error indices were used to examine the performance of models.

2. Materials and Methodology

2.1.Initial dataset providing

The Kuala Lumpur's transport lines to control the congestion, named Klang Valley Rapid Transit System (KVMRT), including a lot of piles for supporting bridges, and is chosen for a research area ofthis study. Fig. 1 shows the position of KVMRT in Malaysia.

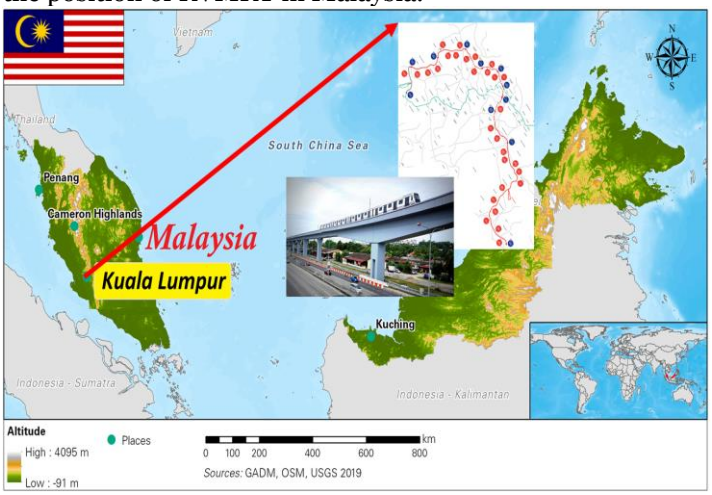

Fig. 1. Transport project of KVMRT location

Several piles are embedded in different rocks, such as phyllite, granite, limestone, and sandstone. The 96 profiles

of the granite-based pile in the present research were gathered to be analyzed. Granites of the San Trias type are found within this area. Subsoil data and materials were acquired from the pile-laying site to identify general geological features. According to the structural results of the basement, it is composed of residual rock. According to the collected data, the bedrock depth ranges from 70 cm underground to over 1400 m. In this regard, the sampling process, related information, and excavation records between piles in the survey area are described.

1- Minimum and maximum UCS values based on ISRM are 25 MPa and 68 MPa, alternatively. [43]

2- Observed rock masses range from averagely weathered rocks to heavily weathered rocks.

3- Subsoil materials are observed in most areas with N_{SPT} values exceeding 50 below per 300 mm at the ground depths of 7.5 to 27.0 m.

4- According to historical data up to a depth of 16.5 MPa, strongly weathered soils are observed. The main soil type consists of hard sand silt with minimum and maximum N_{SPT} of 4 and 167 lower per 300 mm alternatively.

Generating the best data set with efficient dependent items has been the first phase to create a framework as being predictive. The indication of the most important factors affecting the model's results is essential. The abovementioned tests were done using a file analysis setting from Pile Dynamic, Inc. It is mentioned earlier that the length and diameter of piles are parameters that affect the magnitude of pile settlement. Thus, parameters are chosen to analyze the effect of pile geometry: the ratio of the pile length in the soil layer to the pile length in the rock layer (Ls/Lr) and the ratio of the total pile length to pile's diameter (Lp/D). In addition, the model input variable of UCS was selected for the prediction of pile settlement due to the influence of UCS. The N_{SPT} was also considered an input representing the state of the soil layer.

Further, the pile load directly affects the settlement amount thus, the ultimate potential bearing (Q_u) of the pile was considered. Overall, five variables were selected as inputs for evaluating pile settlement (PS). Table 1 shows the inputs and output of the model selected in the study, plus their amplitude. Also, the bar chart of the inputs and target (PS) are illustrated in Fig. 2 with the normal distribution curve of the dataset.

Characteristics of 96 piles constructed by granite rock-based have considered in this research. The the San Trias type of granite rock was seemed in the area. Data and beneath the ground materials at the pile site covered the dominating geological properties. The beneath soil layers are collected from remaining pieces of rocks as in the results. Accordingly, in the data gathered, the bed rock depth is estimated to be in a span of 70 cm to more than the threshold of 1400 m below. Besides, the process of sampling and information of socketed pillar have brought in the lines as follow:

a) The mass of observed rocks among moderately to extremely weathered ones
b) Undermost and top rates of UCS according to the ISRM parameter, respectively, at the level of 25 and 68 Mega Paskal, [41].
c) Log data of bore in the 16.5 meters, extremely weathered soil, and the dominant sort of soil is made up of mostly mud including sand plus a atleast and atmost 4 and 167 of N_{SPT} lower per 300 mm, respectively.
d) A large region under the surface depth in the range between 7.5 and 27.0 meters, underground context with N_{SPT} rate further than 50 deep per 300mm.

Preparing initial information with entering inputs seems the primitive phase for estimating the outputs. Determining the factors impacting the model output is compulsory to the proposed framework. The empirical expriments abovementioned were done by Dynamic of Pile, Inc, applying a pile analysis. It was also previously noted that length of pile and crosssection pile diameter are the variables for the forcasting of pile movement quantity in the pile movement. Therefore, both variant, called the length of pile below the soil to length of pile under the rock proportion (L_s/L_r), and the total length of pile-to-pile diameter (L_p/D) got opted to investigate the status of geometryof pile on settlement. The magnitude of N_{SPT} was similarly was enrolled entring input to demonstrate the status of the soil. Further, the parameter of UCS was considered as input of the model for pillar movement estimation. In addition, the load over pile has a straight effect on the pile movement.Therefore, the last bearing capacity of pile (Q_u) got recognized entering data. variables got opted for appraising pile settlement (PS). The entering data and outcomes from the model in this study, align with revealed ranges, have being indicated by Table 1. The graphs of entering data and target (PS) have been brought through Fig. 2 as well.

Table 1. The dataset used in models, inputs, and target values

Item	Symbol	Unit	Unit.	Max	Min.	S. deviation	Average
The ratio of pile length to diameter	L_p/D	-	6	31.5	4.33	6.557	15.37
Pile settlement	PS	mm	95	20.0	4.494	3.690	10.99
Uniaxial compressive strength	UCS.	MPa	89	68.4	25.324	12.442	43.411
Test of standard penetration	N	-	42	166.	2.92	59.08	80.03
Ultimate potential bearing	Q_u	KN	01	427	12409	803	2454
Soil length to socket length ratio	L_s/L_r	-	14	31.7	0.286	6.562	7.063

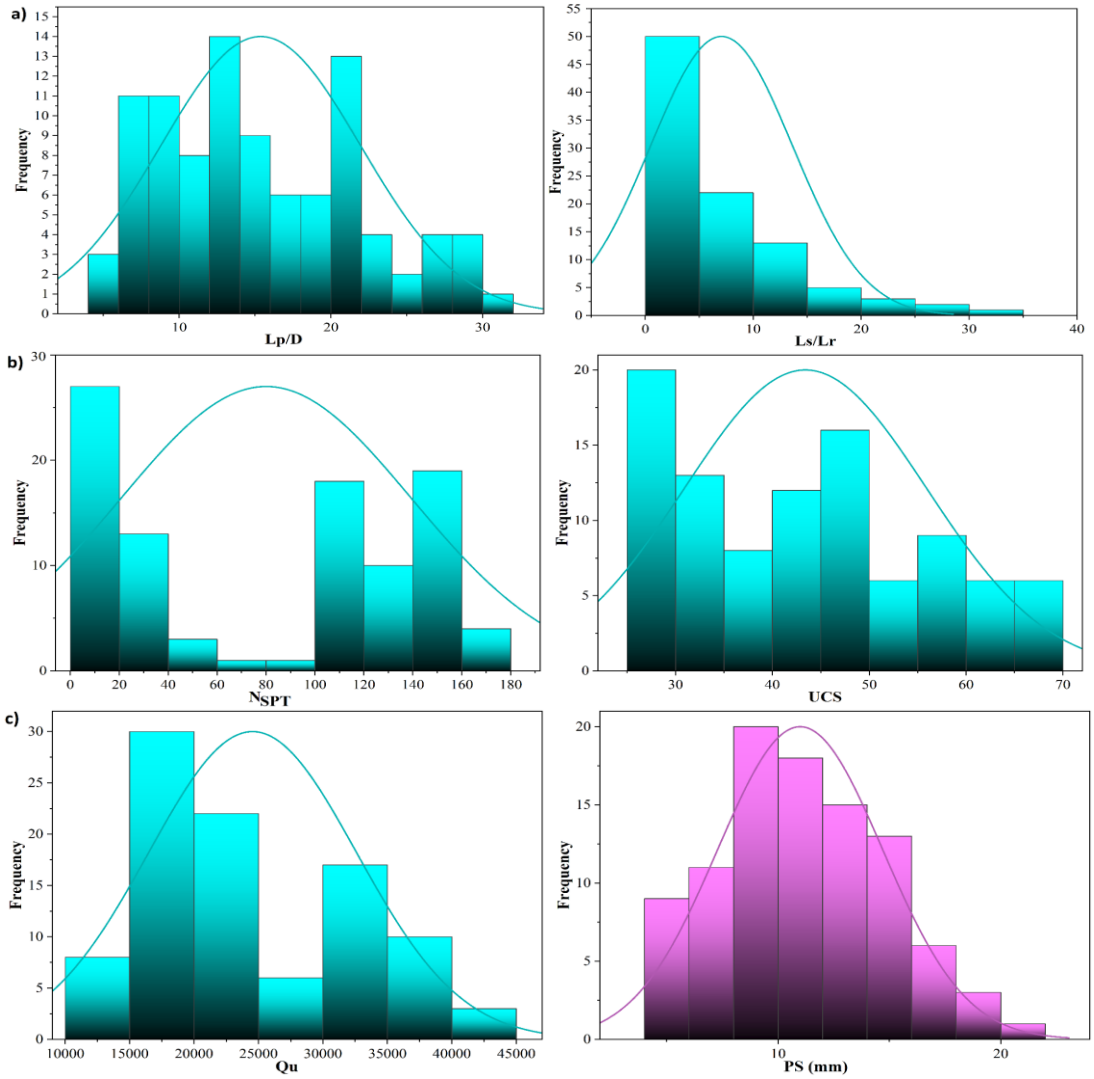

Fig. 2. The input and target bar charts: a) L_p/D and L_s/L_r, b) N_SPT and UCS, c) Q_u and PS

2.2. *Support vector regression, SVR*

The machine learning technique of SVR was presented to categorize the issues of regression [44]. Support vector regression implied the regression sort of support vector machine, which utilizes an area of tolerance (ε) for outlining regression. The categorizing regression classes in the approach SVR are used to create an optimized hyper-plane. SVR has belonged via the learning techniques (supervised) to find responses for issues related to regression and the working out the following function[45].

$$min_{w,b} = \frac{1}{2}\|w\|^2 + C\sum_{i=1}^{m}(\xi_i + \xi_i^*)$$
$$s.t. \quad \begin{Bmatrix} y_i - (w^T x_i + b) \le \varepsilon + \xi_i \\ (w^T x_i + b) - y_i \le \varepsilon + \xi_i^* \\ \xi_i, \xi_i^* \ge 0 \end{Bmatrix} \quad (1)$$

In this equation, ξ, C, w, b, and ε, represent the amount of boundary violation, regularizing variables in the queue, the factor weight, bias, and the rate of deviation from the hyper-plane alternatively. The function of fitness encompasses 2 terms:

$$\frac{1}{2}\|w\|^2 \quad (2)$$

$$C\sum_{i=1}^{m}(\xi_i + \xi_i^*) \quad (3)$$

To enhance the area between the samples and the hyperplane, Eq. (2) was proposed, and conserving the interval between samples with the hyperplane via a unit Eq. (3) played the role of an adjusting tool. The suitable magnitudes of w and b were collected over working out the function as the target for a hyperplane. In the present research, the objective function of the quadratic type is used to generate desirable outcomes [46]. The SVR's essential duty is to solve the determinative parameters at optimal levels:$sigma, \varepsilon$, and C. To find these parameters, diverse frameworks have been employed, wherein optimization algorithms in the present article as HGSO and PSO were joint with SVR to appraise the parameters optimally. The required$sigma,\varepsilon$, and C for dataset guide to coefficients at maximum levels.

2.3. *Particle Swarm Optimization, PSO*

Particle Swarm Algorithm (PSO) has been considered a population basis method. The solution is created over the relationship feedback of separate animal groups. Firstly, the present solution was developed via Kennedy et al. (1995) [47] as well as widely were undertaken by several studies [48–51]. For mentioned solution, the velocity and location seem to be the main population parameters for regulation. Ranking tools scored either component's best location or the overall best solution as the global best solution. The velocity and location of particles are upgraded in iterations to get the maximum number of iterations. Eq. (4) and (5) upgrade the location and velocity.

$$P.v_{ij}^{new} = WP.v_{ij}^{current} + C_1 r_1 (P.p.best_{ij}^{new} - P.p_{ij}^{current}) + C_2 r_2 (Global.best_{ij}^{current} - P.p_{ij}^{current}) \quad (4)$$

$$P.p_{ij}^{new} = P.p_{ij}^{current} + P.v_{ij}^{new} \quad (5)$$

Wherein C_1 plus C_2 denote, respectively, the local and global learning acceleration factors. W show the coefficient inertia. The velocity and the location of the particle are shown by $P.v$ and $P.p$. The parameters of r_1 and r_2 as random numbers are between [0 to 1]. All the swarms' appropriate solutions are denoted by $lobal.best$. The mechanism of search in this algorithm is presented in Fig.3.

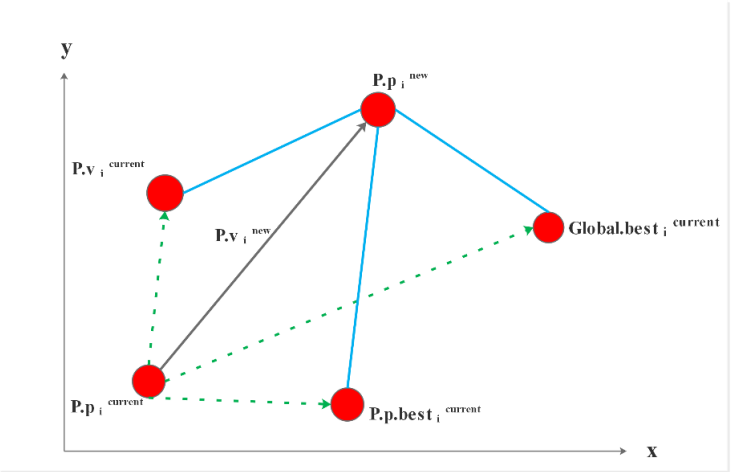

Fig. 3. Search mechanism of Particle Swarm Optimization

2.4. Henry's Gas Solubility Optimization, HGSO

Henry's gas solubility algorithm (HGSO)defines the maximum dissolved solute in a certain solvent value at assumed pressure and temperature levels [40]. Over the law, demonstrating the low-soluble gases solubility in a specific liquid is possible. The pressure and temperature seem efficient items of solubility capacity. The gas solubilities reduce with the incremental temperature variable, whereas the interaction is defined straight for dissolved solids. For pressure, any increase in it causes solubility enhancement [52]. In one study [53], the HGSO algorithm was introduced to consider the gases and their solubility, which the main principles are presented in the following.

i) Defining the location and amount of gases (producing initial population).

ii) Generating the clusters of population basis for the characteristics of the gases.

iii) Specify the clusters' costs, then select and score the best one to specify the best conditions.

iv) Upgradig the Henry coefficients.

$$H_j(t+1) = H_j(t) \times e^{\left(-C_j\left(\frac{T^{\theta}-T(t)}{T(t)\times T^{\theta}}\right)\right)} \quad (6)$$

$$T(t) = e^{\left(\frac{t}{iter}\right)} \quad (7)$$

Wherein the parameter of H_j is the Henry coefficient of j cluster. t And $iter$ denote the temperature and iteration number in the queue. T^{θ} And C_j represent the fixed and random number of zero to one, respectively.

v) Updating the solubility by Eq. (8).

$$S_{i,j}(t) = K \times H_j(t+1) \times P_{i,j}(t) \quad (8)$$

In which, $S_{i,j}$ and $P_{i,j}(t)$ shows the gas solubility and the pressure i of j cluster, alternatively, as well as$K$, a fixed number.

i) Finally, the first location of the population is upgraded by the Eq. (9) and (10).

$$X_{i.j}(t+1) = X_{i.j}(t) + F \times r \times \gamma \times \left(X_{i.best}(t) - X_{i.j}(t)\right) + F \times r \times \alpha \times \left(P_{i,j}(t) \times X_{best}(t) - X_{i,j}(t)\right) \quad (9)$$

$$\gamma = \beta \times e^{\left(-\frac{F_{best}(t)+\varepsilon}{F_{i,j}(t)+\varepsilon}\right)} + \varepsilon \quad (10)$$

Wherein the variable $X_{i,j}$, $X_{i,best}$, X_{best}, F_{best}, $F_{i,j}$, r, are the position of gas i in j cluster, the best gas in j cluster, the best gas in the population, the best cost in the population, gas i in cluster j, a random number in zero to one, respectively. The parameters of α, β, and ε are fixed numbers that α and β is 1 and ε is 0.05. The variable of γ also shows the capability of gases interaction.

vi) The number of worst-cost gases is computed to skip trapping in local minimums.

$$N_w = N \times (rand(C_2 - C_1) + C_1) \quad (11)$$

That N denotes population. C_1 and C_2Constant, respectively, equal to 0.1 and 0.2.

vii) The location of the worst-gas is upgraded in Eq. (12).

$$G_{i,j} = G_{Min(i,j)} + r \times \left(G_{Max(i,j)} - G_{Min(i,j)}\right) \quad (12)$$

Wherein the variable of $G_{i,j}$ shows the location of gas i in cluster$j$. And the variables of G_{Max} and G_{Min} show the maximum and minimum boundaries, alternatively.

2.5. Criteria for evaluation of developed SVR-HGSO and SVR-PSO

The criteria for evaluating models' performance have been brought up in Table 2.

Table 2. Indices employed for the examination of models

Indicator	Symbolism	Equation	status
Pearson's correlation coefficient	R^2	$\left(\frac{\sum_{n=1}^{N}(t_n-\bar{t})(p_n-\bar{p})}{\sqrt{[\sum_{n=1}^{N}(t_n-\bar{p})^2][\sum_{n=1}^{N}(p_n-\bar{p})^2]}}\right)^2$	High value is desirable
Variance account factor	VAF	$\left(1-\frac{var(t_n-y_n)}{var(t_n)}\right)*100$	High value is desirable
Aggregated statistical parameter of the RMSEs, MAEs, and R^2	OBJ	$\left(\frac{n_{train}-n_{test}}{n_{train}+n_{test}}\right)\frac{RMSE_{train}+MAE_{test}}{R^2_{train}+1} + \left(\frac{2n_{train}}{n_{train}+n_{test}}\right)\frac{RMSE_{test}-MAE_{test}}{R^2_{test}+1}$	The low value is desirable [54]

Mean absolute error	*MAE*	$\frac{1}{N}\sum_{n=1}^{N}\lvert p_n - t_n\rvert$	The low value is desirable
Root mean squared error	*RMSE*	$\sqrt{\frac{1}{N}\sum_{n=1}^{N}(p_n - t_n)^2}$	The low value is desirable

In the abovementioned relations, p_N represents the magnitude of PS predicted; t_n shows the n^{th} target value; $\bar{t}$ is the measured averaged data; $\bar{p}$ play the role of the averaged target values that are predicted. Moreover, the variables of the $n_{training}$ and $n_{testing}$ denote the collected number of pile relevant steps of train or test.

2.6. *Designing the hybrid SVR-HGSO and SVR-PSO models*

Coupling the SVR including with arbitrary kernels were defined using optimization algorithms of to find the optimal rates of internal parameters of predictor model containing C, ε, and ξ. Henry's Gas Solubility Optimization (HGSO) and Particle Swarm Optimization (PSO).

3. Results and discussions

Results of SVR, as the models of SVR-HGSO, and SVR-PSO, which are developed machine learning techniques for predicting pile settlement rates, were obtained, and they are presented in this section. So, modeling intricacy and costs are taken into account, which entails increasing the accuracy of the PS estimation, and mentioned items must be figured out considering the optimizers used in this study. Simulations are performed in MATLAB. A detailed diagram of the measured pile settlement ranges for the project used as a study area, KVMRT, is presented in Fig. 4, wherein 70% and 30% of collected data were entered in terms of, respectively, training and testing phases.

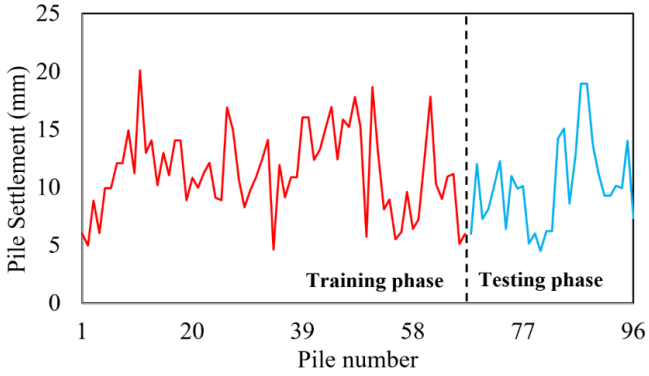

Fig. 4. Measured settling piles data of KVMRT project

SVR-HGSO simulation was performed to estimate the settlement rate of each pile. Those outcomes are shown in Fig. 5. Generally, the estimation process was performed in the desired way defined by the indexes of *RMSE*, and R^2 was obtained 0.288 and 0.997 mm. Also, the best-fit trendline indicates the corresponding modeling accuracy near the dotted bisector, overestimating for settling piles around the 11 mm and underestimating relevant values above this. The best-fit trendline slant of 0.94 also shows proper modeling using the optimization algorithm of HGSO.

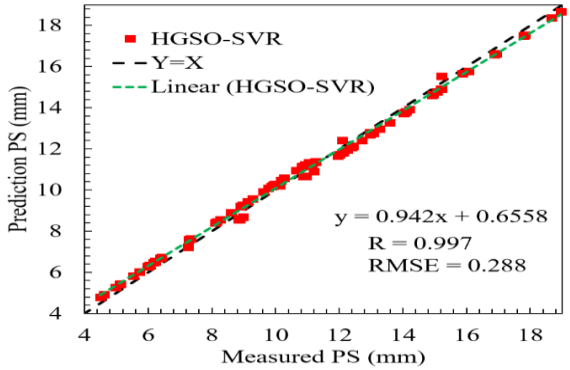

Fig. 5. The SVR-HGSO predicted and measurement pile motion

Similarly, the SVR-PSO outcomes are shown in Fig. 6. The estimation operation is carried out in the desired way, clearly defined by the *RMSE* and R^2 with 0.462 and 0.992 mm. Also, the suitable trendline represents the corresponding simulation accuracy near the dotted bisector, overestimating the settling piles around 11 mm and underestimating PS values above this magnitude. The best-fit trendline slant of 0.94 also shows proper modeling using the optimization algorithm of PSO.

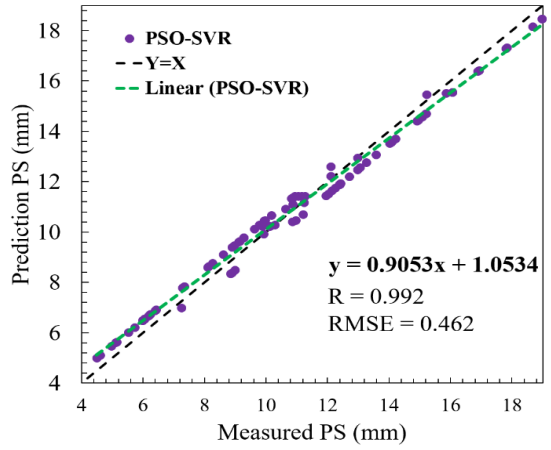

Fig. 6. The SVR-PSO predicted and measurement pile motion

According to Fig. 5 and 6, in comparison with each other, the model of SVR-HGSO acted by better values of *RMSE* and R^2 than SVR-PSO as being 60.71% and 0.52%, respectively. In optimization progress, the HGSO model was fulfilled fine, as seen from the scattered points near the fitting line compared to points in PSO. Especially the high number of piles was considered near the in-situ measurement and the minimum error. Such an event can be discussed in that 70 percent of collected information is applied to train the model.

Table 3 shows the simulation functionality for each model with the criteria of R^2, RMSE, *MAE, OBJ*, and *VAF*. The training and test results indicate the same rates for R^2. The HGSO optimizer outperformed better than PSO for the training phase, which is definite via error criteria. However, the *VAF* shows the identical performance for both models with 0.10 and 0.12 percent difference in training and testing phases, *MAE, RMSE,* and *OBJ* are indicating the remarkable discrepancy for modeling the pile settlement. For the training phase, the *RMSE* index has indicated a great difference of 60.36 %, which is true for the remaining indexes. *MAE* metric also indicates the large gap of 57.41% between the two proposed models in favor of SRV-HGSO with the value of 0.283mm. Identically, the *OBJ* index showed that SRV-PSO with 0.445mm error had appraised the PS values with low-quality magnitudes, while HGSO has gained the 0.284mm as the mistake rate for the abovementioned purpose.

Table 3. Results of models' assessment

			SVR-PSO	SVR-HGSO	Difference (%)
Criteria used	Train step	R^2	0.99	0.996	0.61%
		RMSE	0.463	0.289	60.36%
		MAE	0.445	0.283	57.41%
		VAF	99.88	99.975	0.10%
	Test step	R^2	0.995	0.998	0.32%
		RMSE	0.461	0.285	61.53%
		MAE	0.438	0.279	57.10%
		VAF	99.849	99.973	0.12%
		OBJ	0.445	0.284	56.67%

For a better view, Fig. 7 has exhibited the difference of modeling two frameworks by dividing the PS rates estimated by SVR-PSO and SVR-HGSO. As shown in Fig.7, there are many times in the diagram that the levels higher or lower than zero line are touched for PS values calculating. While the outstanding difference in error criteria of Table 3 could lead us to understand that the SVR-HGSO has modeled the PS values with a so much difference rather than SVR-PSO. The little scale of error, such as 0.1 millimeter in pile settlement, is not the reason for the large distance in the results of models. That Fig. 7 proves this fact with the nearly symmetric error condition.

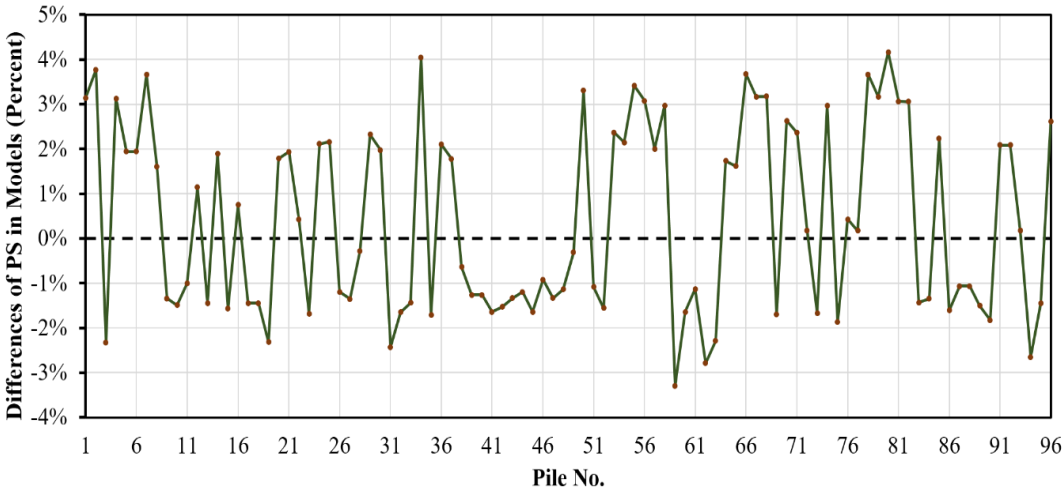

Fig. 7. The discrepancy in PS values computed by SVR-PSO and SVR-HGSO

To get a definite idea of the accuracy in the simulation, Fig. 8 wants to show the simulation error for each pile compared to the values as targets. With Fig. 8, multiple cases are observed wherein the measured values and those of proposed models do not match. As can be realized in both testing and training phases, much of the simulation is done right. This figure shows which pile and how significant the deviation exists between the model and the in-situ data.

Fig. 8. PS simulated and measured modeling with: (a) SVR-HGSO and (b) SVR-PSO

The SVR-HGSO (a) was simulated adjacent to the field measurements seen in the figure. However, for piles number 24 and 25, the discrepancy between measurement and modeling is greater than other points. In the same way, this story works for SVP-PSO (b). The simulation accuracy is better improved by passing the dotted line as the boundary of the test and training phases.

Fig. 9 tries to enlarge the gaps of PS magnitudes modeled and measured in Fig.8. Practically, Fig. 9 represents the error in goal achievement for the simulated piles as to be overestimated (positive) or underestimated (negative). Therefore, based on Fig. 9 (a), when SVR-HGSO models the movement of the pile in the training stage, it can be seen that the errors all over the plot exist with a high value of

11percent. Also, this matter runs similarly for the test stage, and there is no constant error distribution pattern. And SVR-HGSO (b) performed an identical operation over simulating settlement of pile associated with a high rate error of 6.7 percent.

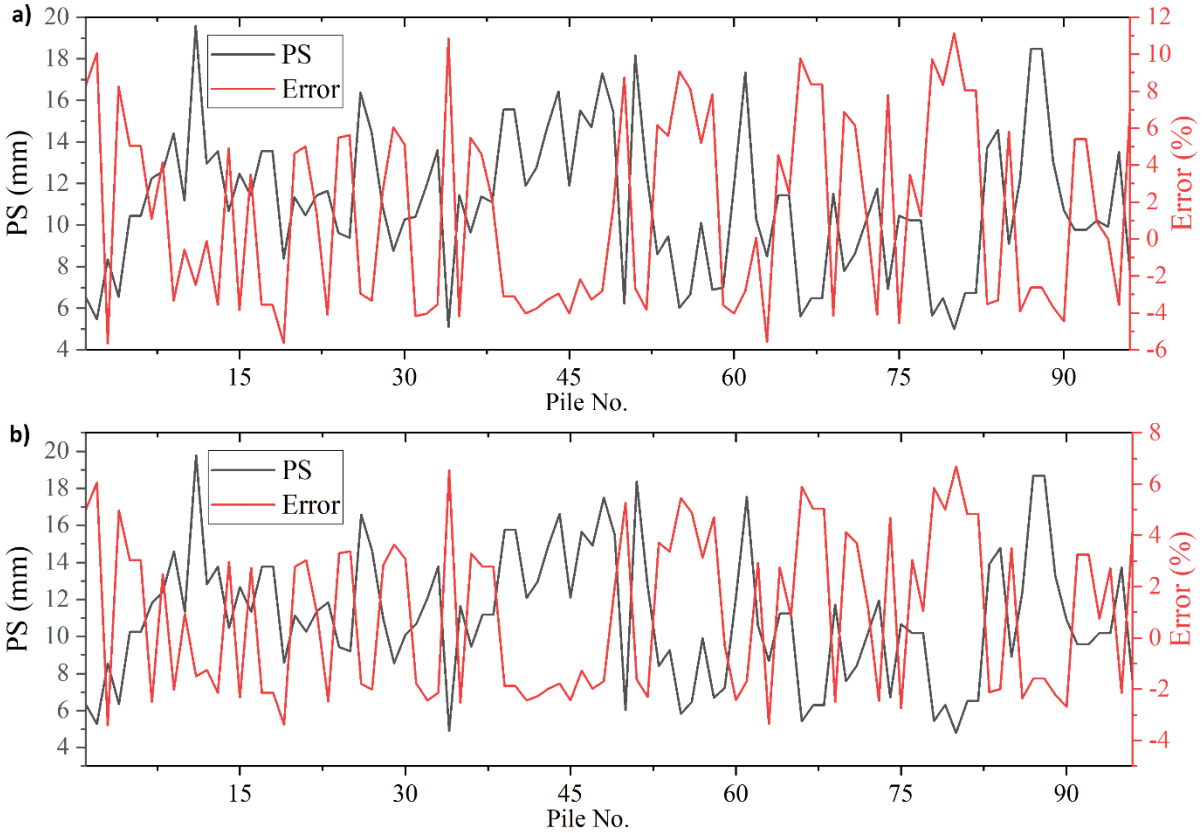

Fig. 9. The PS estimated values against the errors in, (a) SVR-PSO, and (b) SVR-HGSO

The present section indicates the normal error distributions of developed models. Fig. 10 monitors the distribution of errors according to their count plus the curve of its normal distribution for SVR-PSO and SVR-HGSO. In this regard, there is no harmonic error distribution for both models. That accumulation of errors around the zero point has led to creating a flat normal distribution error curve. The concentration of the SVR-HGSO model is better distributed as near-zero than the other one with a flatter curve. To sum up, the HGSO has performed fine instead of PSO based on the indicators and diagrams shown in this section.

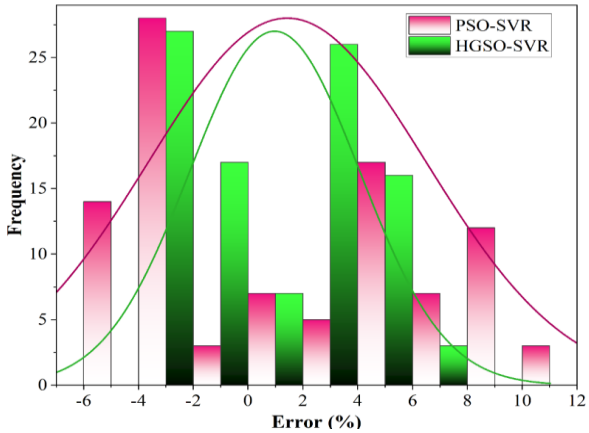

Fig. 10. Error distribution in SVR-HGSO model

4. Conclusions

Ensuring constructional projects are safe, as stacked structures, requires consideration to immunize structures over the period. Pile settlement is an important project problem and is receiving a lot of attention to prevent failure before construction operations. Several items for estimating pile motion can help understand the project's perspective during the loading phase. Most smart strategies for the mathematical calculation of pile movement are used in PS simulations. Thus, in this study, we proposed to operate support vector regression together with henry's gas solubility optimization and particle swarm optimization for accurate pile motion calculation. The Kuala Lumpur transportation network was selected to study the movement of piles based on the land rock characteristics using the developed SVR-HGSO and SVR-PSO structures. With five metrics used in evaluating the performance of each model, we will be able to reduce the cost and energy to be aware of any pile motion to avoid heavy failure. Based on indicators, the SVR-HGSO could better model the pile motion rates than SVR-PSO. Both models had identical performances on a millimeter-scale of 0.1 except for R^2 and VAF indices. Other error criteria showed the great mistake over the modeling process. In this regard, the training phase *RMSE* index indicated a great difference of 60.36 % in favor of SVR-HGSO. *MAE* metric also showed a large gap of 57.41% between the two proposed models in favor of SRV-HGSO with the value of 0.283mm. Identically, the *OBJ* index, by encompassing RMSE and MAE of training and testing phases, showed that SRV-PSO with 0.445mm error had appraised the PS values with low-quality magnitudes, while HGSO has gained the 0.284mm as the mistake rate for the abovementioned purpose. Finally, the HGSO has performed fine rather than PSO however, both have had maximum error rates of 6.7 and 11.14 percent. Generally, according to the results of developed frameworks, estimation of pile settlement using SVR coupled with optimization algorithms were done successfully. Nevertheless, employing the hybrid models with desirable outcomes with the aid of smart software-based approaches can reduce the costs of physical experiments and simultaneously increase the accuracy of predicting mechanical features of crucial concrete material.

REFERENCES

[1] H.G. Poulos, Pile behaviour—theory and application, Geotechnique. 39 (1989) 365–415.

[2] M.F. Randolph, Science and empiricism in pile foundation design, Géotechnique. 53 (2003) 847–875.

[3] H.G. Poulos, Pile group settlement estimation—Research to practice, Found. Anal. Des. Innov. Methods. (2006) 1–22.

[4] D.P. Stewart, R.J. Jewell, M.F. Randolph, Design of piled bridge abutments on soft clay for loading from lateral soil movements, Geotechnique. 44 (1994) 277–296.

[5] J. Cherian, Determining the amount of earthquake displacement using differential synthetic aperture radar interferometry (D-InSAR) and satellite images of Sentinel-1 A: A case study of Sarpol-e Zahab city, Adv. Eng. Intell. Syst. 1 (2022).

[6] Z. Nurlan, A novel hybrid radial basis function method for predicting the fresh and hardened properties of self-compacting concrete, Adv. Eng. Intell. Syst. 1 (2022).

[7] H. Cheng, S. Kitchen, G. Daniels, Novel hybrid radial based neural network model on predicting the compressive strength of long-term HPC concrete, Adv. Eng. Intell. Syst. 1 (2022).

[8] Q. Zhang, M. Afzal, Prediction of the elastic modulus of recycled aggregate concrete applying hybrid artificial intelligence and machine learning algorithms, Struct. Concr. (2021).

[9] L. Huang, W. Jiang, Y. Wang, Y. Zhu, M. Afzal, Prediction of long-term compressive strength of concrete with admixtures using hybrid swarm-based algorithms, Smart Struct. Syst. 29 (2022) 433–444.

[10] R.S. Benemaran, M. Esmaeili-Falak, Optimization of cost and mechanical properties of concrete with admixtures using MARS and PSO, Comput. Concr. 26 (2020) 309–316.

[11] R. Sarkhani Benemaran, M. Esmaeili-Falak, A. Javadi, Predicting resilient modulus of flexible pavement foundation using extreme gradient boosting based optimized models, Int. J. Pavement Eng. (2022). https://doi.org/10.1080/10298436.2022.2095385.

[12] R. Sarkhani Benemaran, M. Esmaeili-Falak, H. Katebi, Physical and numerical modelling of pile-stabilised saturated layered slopes, Proc. Inst. Civ. Eng. Eng. (2020) 1–16.

[13] H.G. Poulos, Tall building foundation design, CRC Press, 2017.

[14] Y. Zhang, X. Hu, D.D. Tannant, G. Zhang, F. Tan, Field monitoring and deformation characteristics of a landslide with piles in the Three Gorges Reservoir area, Landslides. 15 (2018) 581–592.

[15] Y. Zhang, D.C. Richardson, O.S. Barnouin, P. Michel, S.R. Schwartz, R.-L. Ballouz, Rotational failure of rubble-pile bodies: influences of shear and cohesive strengths, Astrophys. J. 857 (2018) 15.

[16] I.-M. Lee, J.-H. Lee, Prediction of pile bearing capacity using artificial neural networks, Comput. Geotech. 18 (1996) 189–200.

[17] W.F. Che, T.M.H. Lok, S.C. Tam, H. Novais-Ferreira, Axial capacity prediction for driven piles at Macao using artificial neural network, (2003).
[18] H. Liu, T.J. Li, Y.F. Zhang, The application of artificial neural networks in estimating the pile bearing capacity, (1997).
[19] A.M. Hanna, G. Morcous, M. Helmy, Efficiency of pile groups installed in cohesionless soil using artificial neural networks, Can. Geotech. J. 41 (2004) 1241–1249.
[20] M. Shanbeh, D. Najafzadeh, S.A.H. Ravandi, Predicting pull-out force of loop pile of woven terry fabrics using artificial neural network algorithm, Ind. Textila. 63 (2012) 37–41.
[21] A.T.C. Goh, Pile Driving Records Reanalyzed Using Neural Networks, J. Geotech. Eng. 122 (1996) 492–495. https://doi.org/10.1061/(ASCE)0733-9410(1996)122:6(492).
[22] M. Pal, S. Deswal, Modelling pile capacity using Gaussian process regression, Comput. Geotech. 37 (2010) 942–947.
[23] P. Samui, Determination of friction capacity of driven pile in clay using Gaussian process regression (GPR), and minimax probability machine regression (MPMR), Geotech. Geol. Eng. 37 (2019) 4643–4647.
[24] E. Momeni, M.B. Dowlatshahi, F. Omidinasab, H. Maizir, D.J. Armaghani, Gaussian process regression technique to estimate the pile bearing capacity, Arab. J. Sci. Eng. 45 (2020) 8255–8267.
[25] W.G. Zhang, A.T.C. Goh, Multivariate adaptive regression splines for analysis of geotechnical engineering systems, Comput. Geotech. 48 (2013) 82–95.
[26] L. Teodorescu, D. Sherwood, High energy physics event selection with gene expression programming, Comput. Phys. Commun. 178 (2008) 409–419.
[27] T.-T. Le, M.V. Le, Development of user-friendly kernel-based Gaussian process regression model for prediction of load-bearing capacity of square concrete-filled steel tubular members, Mater. Struct. 54 (2021) 1–24.
[28] I. Alkroosh, H. Nikraz, Correlation of pile axial capacity and CPT data using gene expression programming, Geotech. Geol. Eng. 29 (2011) 725–748.
[29] A. Mollahasani, A.H. Alavi, A.H. Gandomi, Empirical modeling of plate load test moduli of soil via gene expression programming, Comput. Geotech. 38 (2011) 281–286.
[30] A. Ozbek, M. Unsal, A. Dikec, Estimating uniaxial compressive strength of rocks using genetic expression programming, J. Rock Mech. Geotech. Eng. 5 (2013) 325–329.
[31] S.R. Dindarloo, Prediction of blast-induced ground vibrations via genetic programming, Int. J. Min. Sci. Technol. 25 (2015) 1011–1015.
[32] S. Alemdag, Z. Gurocak, A. Cevik, A.F. Cabalar, C. Gokceoglu, Modeling deformation modulus of a stratified sedimentary rock mass using neural network, fuzzy inference and genetic programming, Eng. Geol. 203 (2016) 70–82.
[33] C.I. Teh, K.S. Wong, A.T.C. Goh, S. Jaritngam, Prediction of pile capacity using neural networks, J. Comput. Civ. Eng. 11 (1997) 129–138.
[34] A. Soleimanbeigi, N. Hataf, Prediction of settlement of shallow foundations on reinforced soils using neural networks, Geosynth. Int. 13 (2006) 161–170.
[35] S. Wang, A. Mathew, Y. Chen, L. Xi, L. Ma, J. Lee, Empirical analysis of support vector machine ensemble classifiers, Expert Syst. Appl. 36 (2009) 6466–6476.
[36] J. Platt, Probabilistic outputs for support vector machines and comparisons to regularized likelihood methods, Adv. Large Margin Classif. 10 (1999) 61–74.
[37] A. Gholampour, I. Mansouri, O. Kisi, T. Ozbakkaloglu, Evaluation of mechanical properties of concretes containing coarse recycled concrete aggregates using multivariate adaptive regression splines (MARS), M5 model tree (M5Tree), and least squares support vector regression (LSSVR) models, Neural Comput. Appl. 32 (2020) 295–308. https://doi.org/10.1007/s00521-018-3630-y.
[38] M. Ayubi Rad, M.S. Ayubirad, Comparison of artificial neural network and coupled simulated annealing based least square support vector regression models for prediction of compressive strength of high-performance concrete, Sci. Iran. 24 (2017) 487–496.
[39] Y. Shi, Particle swarm optimization: developments, applications and resources, in: Proc. 2001 Congr. Evol. Comput. (IEEE Cat. No. 01TH8546), IEEE, 2001: pp. 81–86.
[40] V. Mohebbi, A. Naderifar, R.M. Behbahani, M. Moshfeghian, Determination of Henry's law constant of light hydrocarbon gases at low temperatures, J. Chem. Thermodyn. 51 (2012) 8–11. https://doi.org/10.1016/j.jct.2012.02.014.
[41] M. Shariati, M.S. Mafipour, B. Ghahremani, F. Azarhomayun, M. Ahmadi, N.T. Trung, A. Shariati, A novel hybrid extreme learning machine–grey wolf optimizer (ELM-GWO) model to predict compressive strength of concrete with partial replacements for cement, Eng. Comput. (2020). https://doi.org/10.1007/s00366-020-01081-0.

[42] M.A. Shahin, H.R. Maier, M.B. Jaksa, Predicting settlement of shallow foundations using neural networks, J. Geotech. Geoenvironmental Eng. 128 (2002) 785–793.
[43] A.W. Hatheway, The complete ISRM suggested methods for rock characterization, testing and monitoring; 1974–2006, (2009).
[44] L. Wang, Support vector machines: theory and applications, Springer Science & Business Media, 2005.
[45] V. Vapnik, The nature of statistical learning theory, Springer science & business media, 2013.
[46] A. Al-Fugara, M. Ahmadlou, A.R. Al-Shabeeb, S. AlAyyash, H. Al-Amoush, R. Al-Adamat, Spatial mapping of groundwater springs potentiality using grid search-based and genetic algorithm-based support vector regression, Geocarto Int. (2020) 1–20.
[47] R. Eberhart, J. Kennedy, A new optimizer using particle swarm theory, in: MHS'95. Proc. Sixth Int. Symp. Micro Mach. Hum. Sci., IEEE, n.d.: pp. 39–43. https://doi.org/10.1109/MHS.1995.494215.
[48] A. Maleki, Optimal operation of a grid-connected fuel cell based combined heat and power systems using particle swarm optimisation for residential sector, Int. J. Ambient Energy. 42 (2021) 550–557. https://doi.org/10.1080/01430750.2018.1562968.
[49] G. Perampalam, K. Poologanathan, S. Gunalan, J. Ye, B. Nagaratnam, Optimum Design of Cold-formed Steel Beams: Particle Swarm Optimisation and Numerical Analysis, Ce/papers. 3 (2019) 205–210. https://doi.org/10.1002/cepa.1159.
[50] F. Masoumi, S. Najjar-Ghabel, A. Safarzadeh, B. Sadaghat, Automatic calibration of the groundwater simulation model with high parameter dimensionality using sequential uncertainty fitting approach, Water Supply. 20 (2020) 3487–3501. https://doi.org/10.2166/ws.2020.241.
[51] M.B. Patil, M.N. Naidu, A. Vasan, M.R.R. Varma, Water distribution system design using multi-objective particle swarm optimisation, Sādhanā. 45 (2020) 21. https://doi.org/10.1007/s12046-019-1258-y.
[52] T.L. Brown, Chemistry: the central science, Pearson Education, 2009.
[53] F.A. Hashim, E.H. Houssein, M.S. Mabrouk, W. Al-Atabany, S. Mirjalili, Henry gas solubility optimization: A novel physics-based algorithm, Futur. Gener. Comput. Syst. 101 (2019) 646–667. https://doi.org/10.1016/j.future.2019.07.015.
[54] G. Pazouki, E.M. Golafshani, A. Behnood, Predicting the compressive strength of self-compacting concrete containing Class F fly ash using metaheuristic radial basis function neural network, Struct. Concr. (2021). https://doi.org/10.1002/suco.202000047.